Electrochemical Biomass Upgrading: Degradation of Glucose to Lactic Acid on a Copper (II) Electrode

Lars Ostervold,[a,b] Sergio I Perez Bakovic[b], Jamie Hestekin*[b] and Lauren Greenlee*[a,b]

[a]*Department of Chemical Engineering, Pennsylvania State University, University Park, PA, USA.*
[b]*Ralph E. Martin Department of Chemical Engineering, Fayetteville, AR, USA. Email:*
**greenlee@psu.edu; jhesteki@uark.edu*

Contents

Supporting Information

XPS Survey Scans

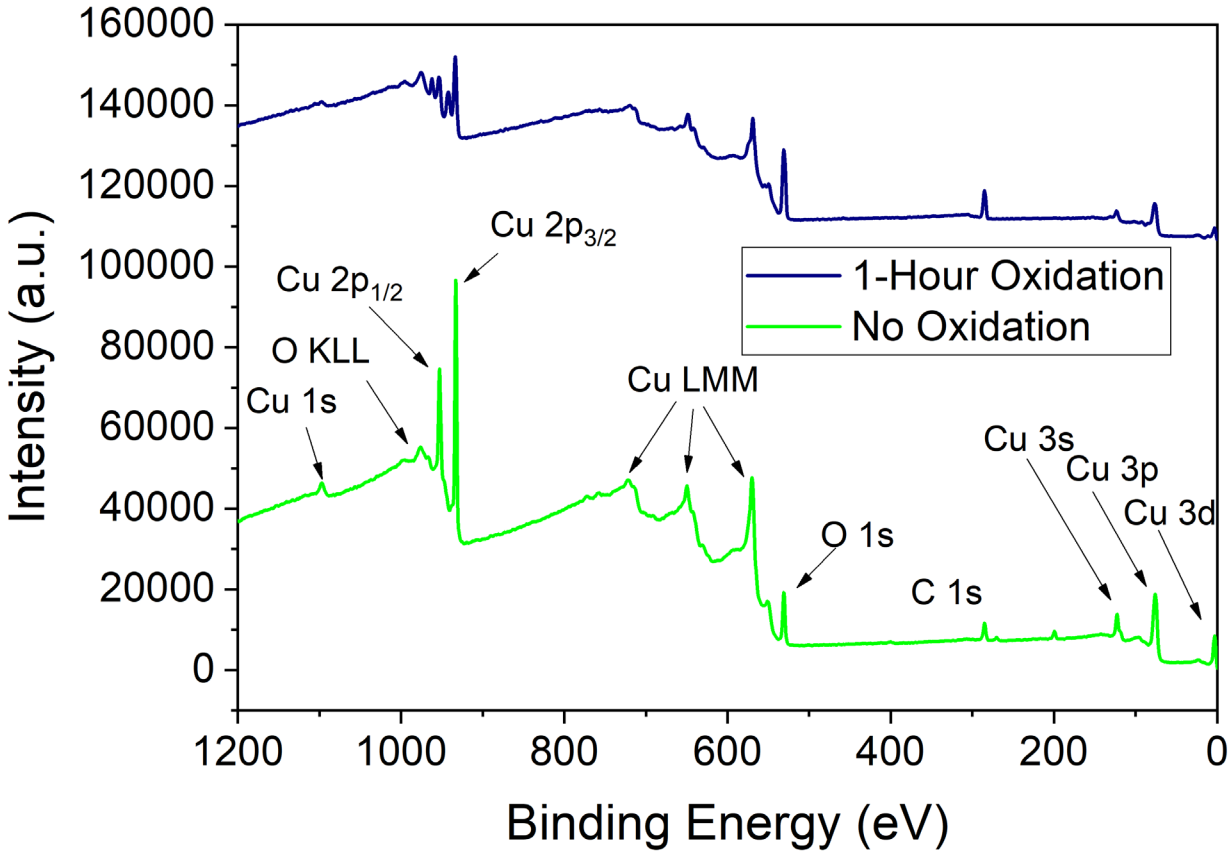

Fig. S1 Survey scans using x-ray photoelectron spectroscopy instrument described in Experimental section of main text. Survey scans for copper electrodes with no electrooxidation (green) and 1 hour of oxidation (blue) are shown.

Peak Fitting for XPS Data

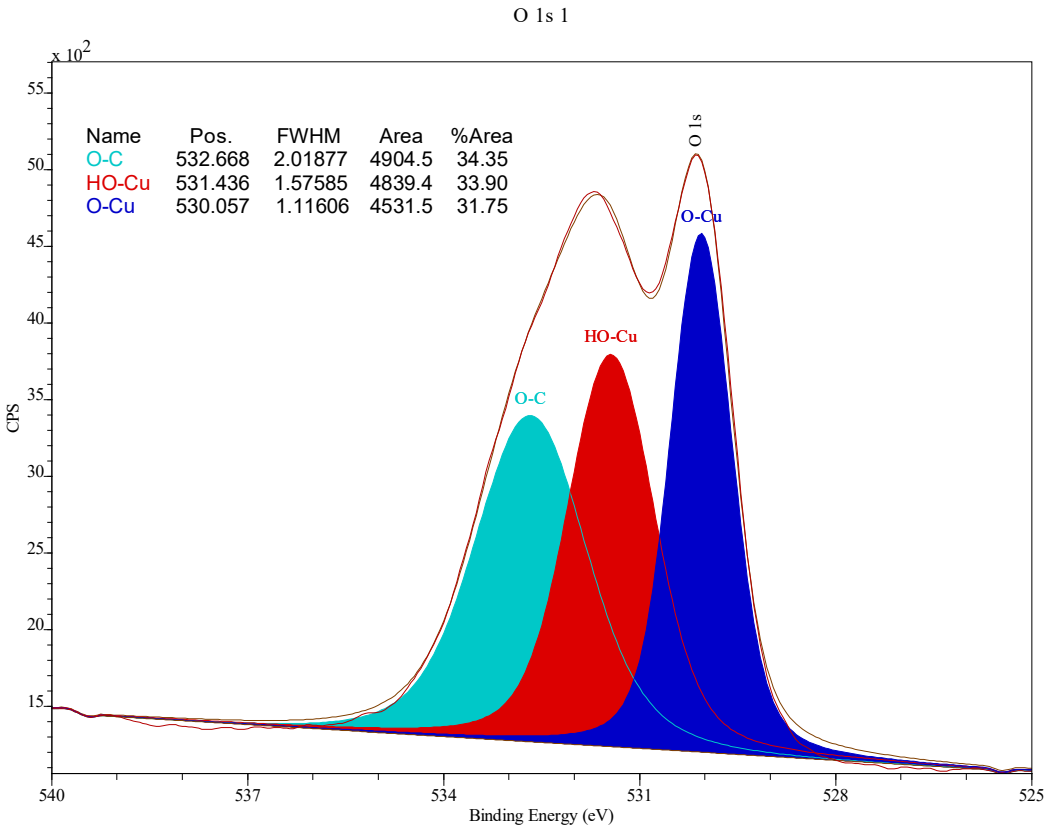

Fig. S2 Peak fitting for copper foil after one hour of electrooxidation

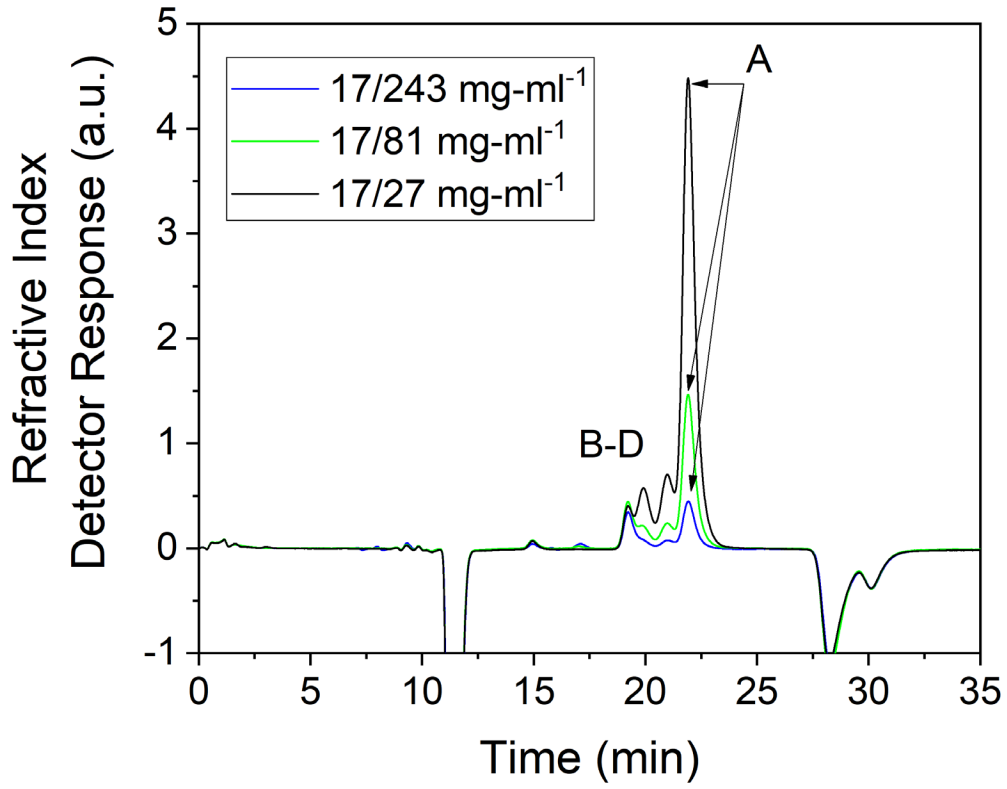

Fig. S3 HPLC chromatogram of lactic acid standard. Other peaks are isomers of lactic acid; quantification was performed based on Peak A. All other peaks shown are system or injection peaks. Peaks B-D are due to racemic mixture of lactic acid while lactic acid produced by the system was of the same form as Peak A, so quantification was performed based on Peak A. All other peaks are system peaks or mobile phase impurities.

Lactic Acid Spike Experiment

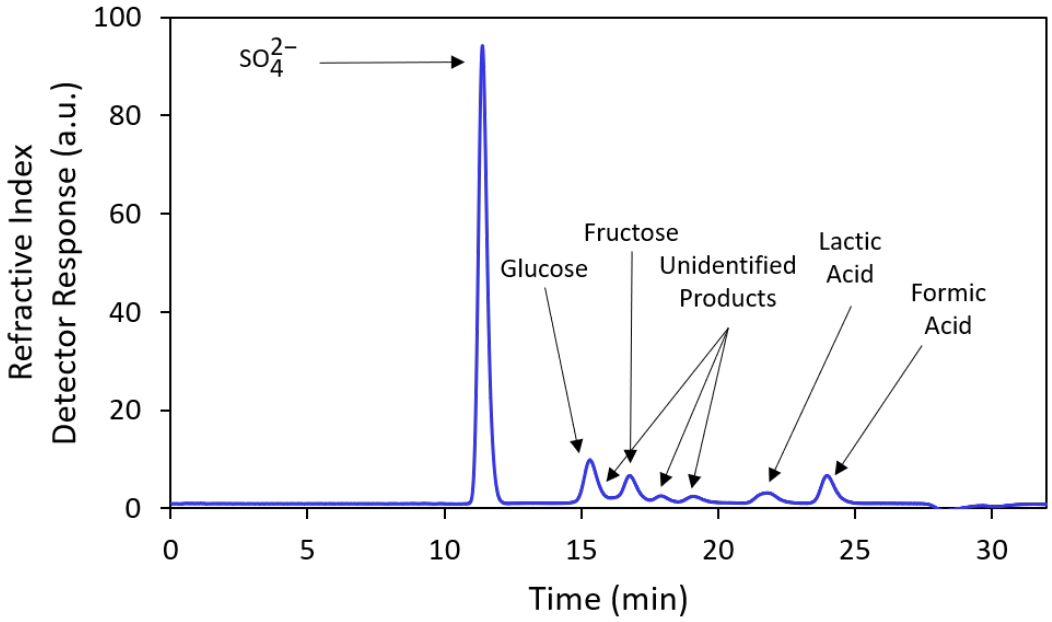

Fig. S4 Full HPLC chromatogram for typical reaction of electrochemical glucose degradation. As discussed in the main text, side products were not identified or quantified because they composed a minority percentage after quantifying four compounds. Lactic acid spike was a racemic mixture, explaining the new peaks that appear.

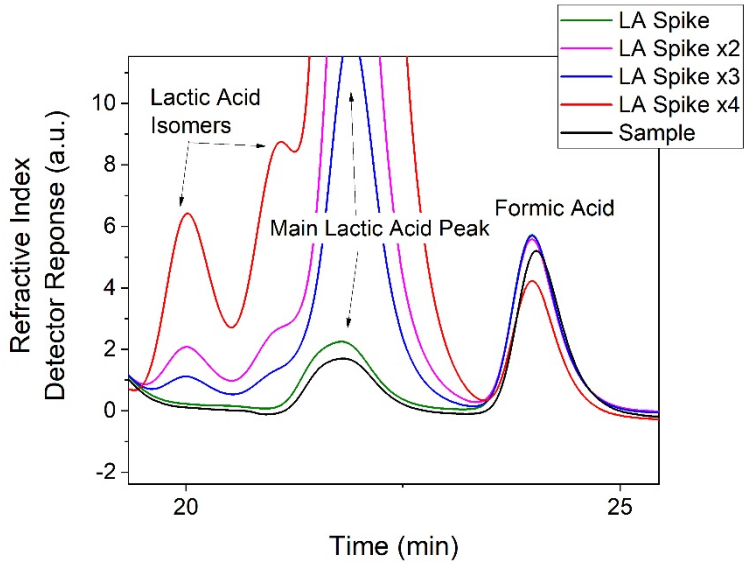

Fig. S5 Zoomed Fig. S4 in on lactic acid peak with spiking of lactic acid standard. Note the sample peak retains shape when minute amount of lactic acid is added. Change in formic acid peak between spike experiments are due to 'bleeding' effects from high concentrations of lactic acid or from homogenous oxidation.

Quantitative Reaction Yield

Table S1 Quantitative data displayed in Fig. 4 (main text)

Condition	Glucose Conversion	Fructose Yield	Lactic Acid Yield	Formic Acid Yield	Lactic Acid Selectivity
1.56V	82.4±2.9%	9.4±1.7%	20.9±0.5%	44.1±2.6%	25.4±1.5%
1.51V	82.6±3.3%	9.0±1.3%	20.9±1.5%	47.8±2.4%	25.3±2.8%
1.46 V	75.0±0.6%	12.5±0.4%	23.3±1.2%	38.4±2.4%	31.1±1.9%
0.5M NaOH	65.4±3.5%	19.1±2.2%	13.5±2.3%	18.2±4.8%	20.8±4.7%
No Oxidation	80.8±0.7%	9.8±0.9%	22.9±1.8%	40.4±1.2%	28.3±2.5%

Time Sampling Data

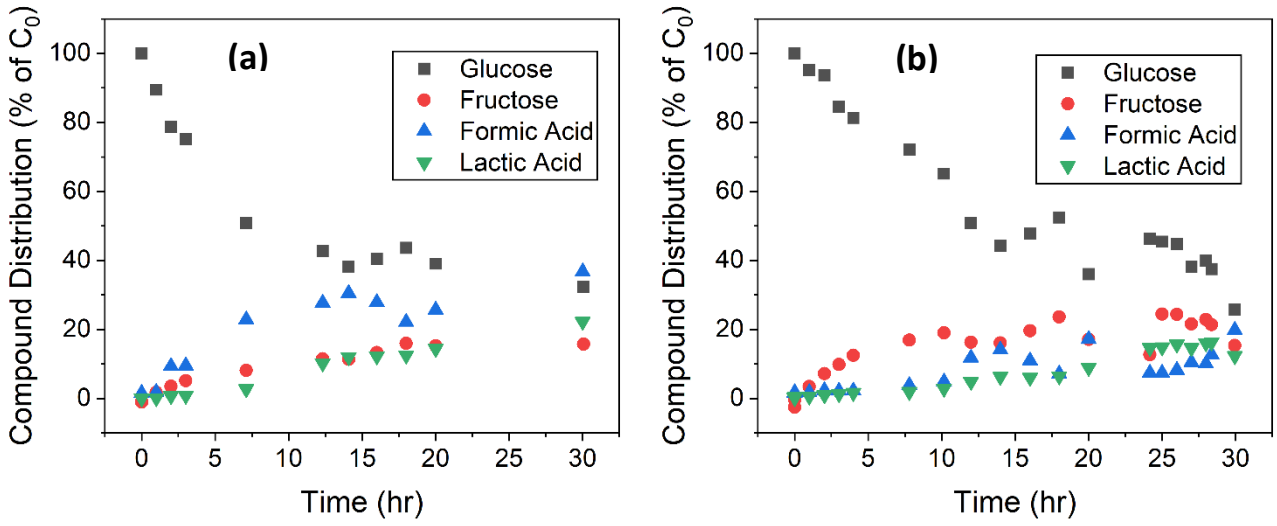

Fig. S6 Data for time sampling taken during reaction for 30-hour potential holds in 1.0 M NaOH (a) and 0.5 M NaOH(b), 0.1 M glucose solutions at 1.46 V vs. RHE. Working electrode was Cu foil (2 cm^2) after being oxidized for 1 hour; reference and counter electrodes were Hg/HgO and platinum coil, respectively.

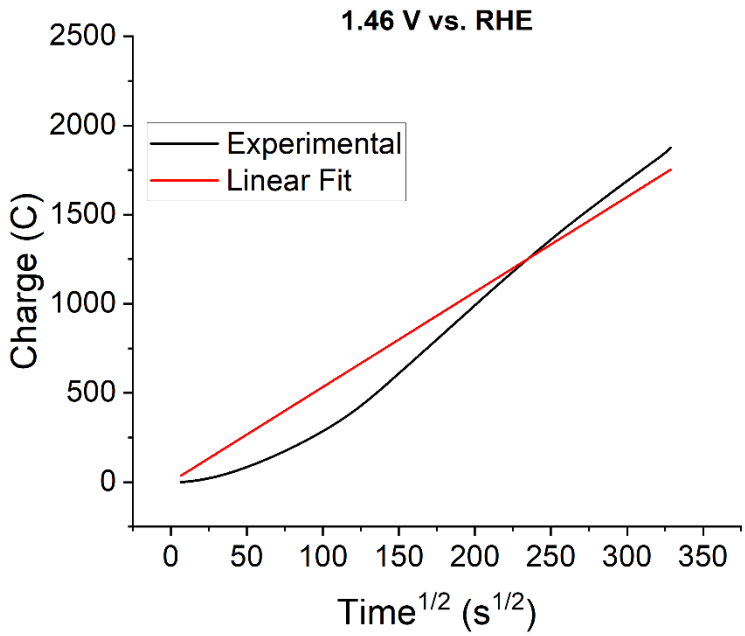

Fig. S7 Integrated Cottrell test performed on a 30-hour potential hold experiment in 1.0 M NaOH, 0.1 M glucose solution. The working electrode was Cu foil (2 cm^2) after being oxidized for 1 hour. The reference and counter electrodes were Hg/HgO and platinum coil, respectively

The charge for a diffusion-controlled system in response to large-amplitude potential step obeys the integrated Cottrell equation (Equation 1).

$$Q_d = \frac{2nFAD_i^{1/2}C_i^* t^{1/2}}{\pi^{1/2}} (1)$$

Equation 1 - The integrated Cottrell equation where Q_d is the charge of a diffusion-limited system, n is the number of electrons per mole of reactant, F is Faraday's constant, D_i is the diffusion coefficient species i (the electroactive spcies), C_i^* is the concentration of i in the bulk solution, and t is time.

If we plot Q_d vs. $t^{1/2}$, the plot should be linear for a diffusion-controlled system. Fig. S7 shows the data do not exhibit a linear behavior with respect to $t^{1/2}$, suggesting the system is not diffusion-controlled. The system should have a linear dependence on the bulk concentration of glucose, which is decreasing over time. To test for kinetic limitations, we look to the Butler-Volmer equation (Equation 2, discussed later). A plot of the ln|i| vs. potential should be linear for a kinetically-limited system. The data in Fig. S8 exhibit a linear behavior on the front edge of the reaction peak in Fig. 2. The deviation from linearity at high potentials is due to other limitations (perhaps mass-transport) and deviation at low potentials is due to insufficient applied energy to cause the reaction. Given the kinetic limitations, the important parameter is activity, which is easily compared through pre- vs. post-reaction cyclic voltammetry experiment.

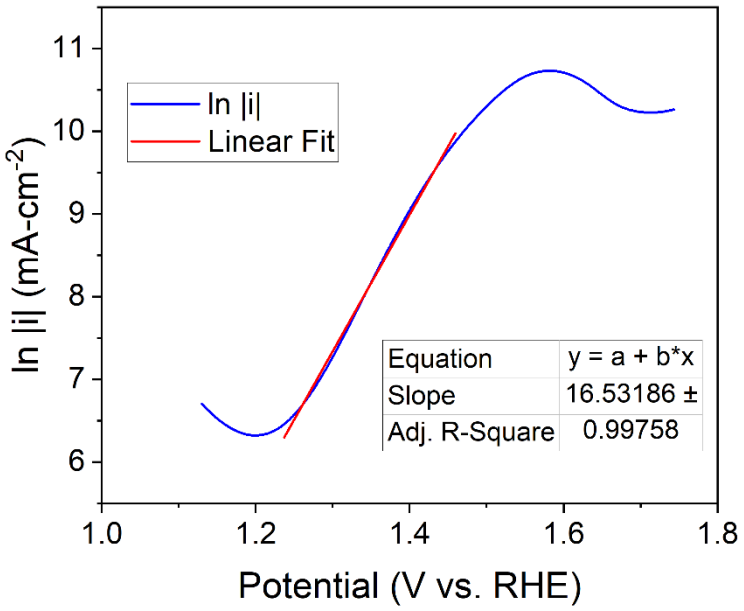

Fig. S8 Electroactive potential region of the ln|i| versus potential for the cyclic voltammetry experiment performed in Fig. 2. The cyclic voltammetry was performed at a scan rate of 50 mV-s^{-1} in 1.0 M NaOH (pH = 13.6) solution with 0.1 M glucose (blue). The working electrode was Cu foil (2 cm^2) after being oxidized for 1 hour. The reference and counter electrodes were Hg/HgO and platinum coil, respectively. Data taken from the 5th cycle.

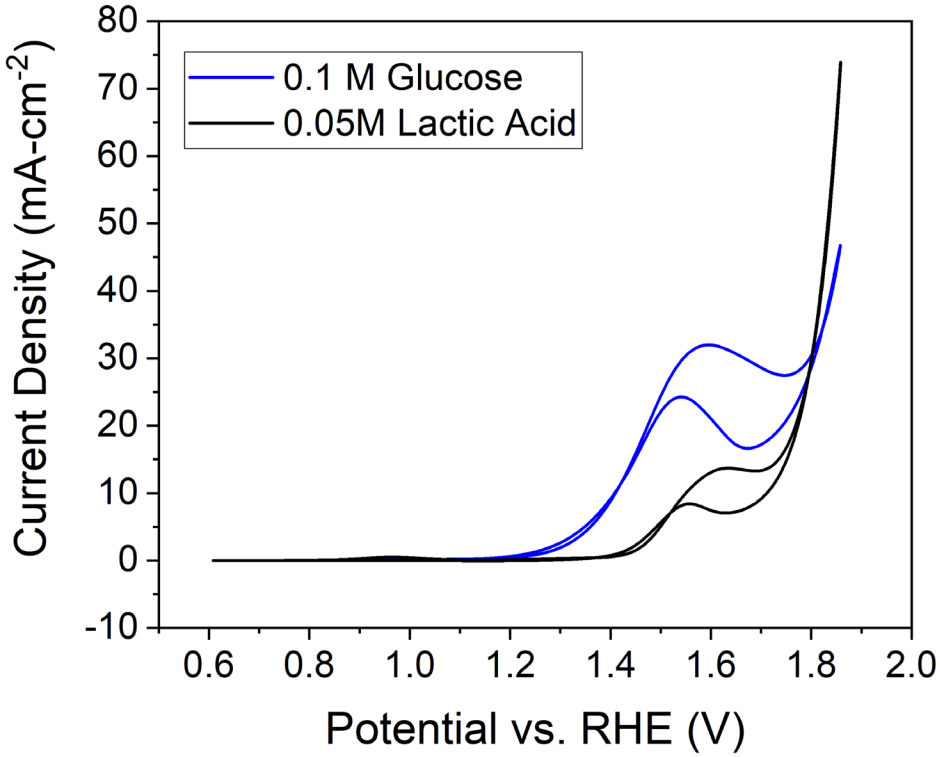

Fig. S9 Cyclic voltammetry performed at a scan rate of 50 mV-s^{-1} in 1.0 M NaOH with 0.1 M glucose (blue) or 0.05 M lactic acid (black). Working electrode was unoxidized Cu foil (2 cm^2) after. Reference and counter electrodes were Hg/HgO and platinum coil, respectively. All sets of data are taken from the 5th cycle of the scan. Lactic acid oxidation peak shifts left compared to glucose oxidation peak as discussed in the Electrode Recyclability section.

All Pre- vs. Post- Reaction Cyclic Voltammetries

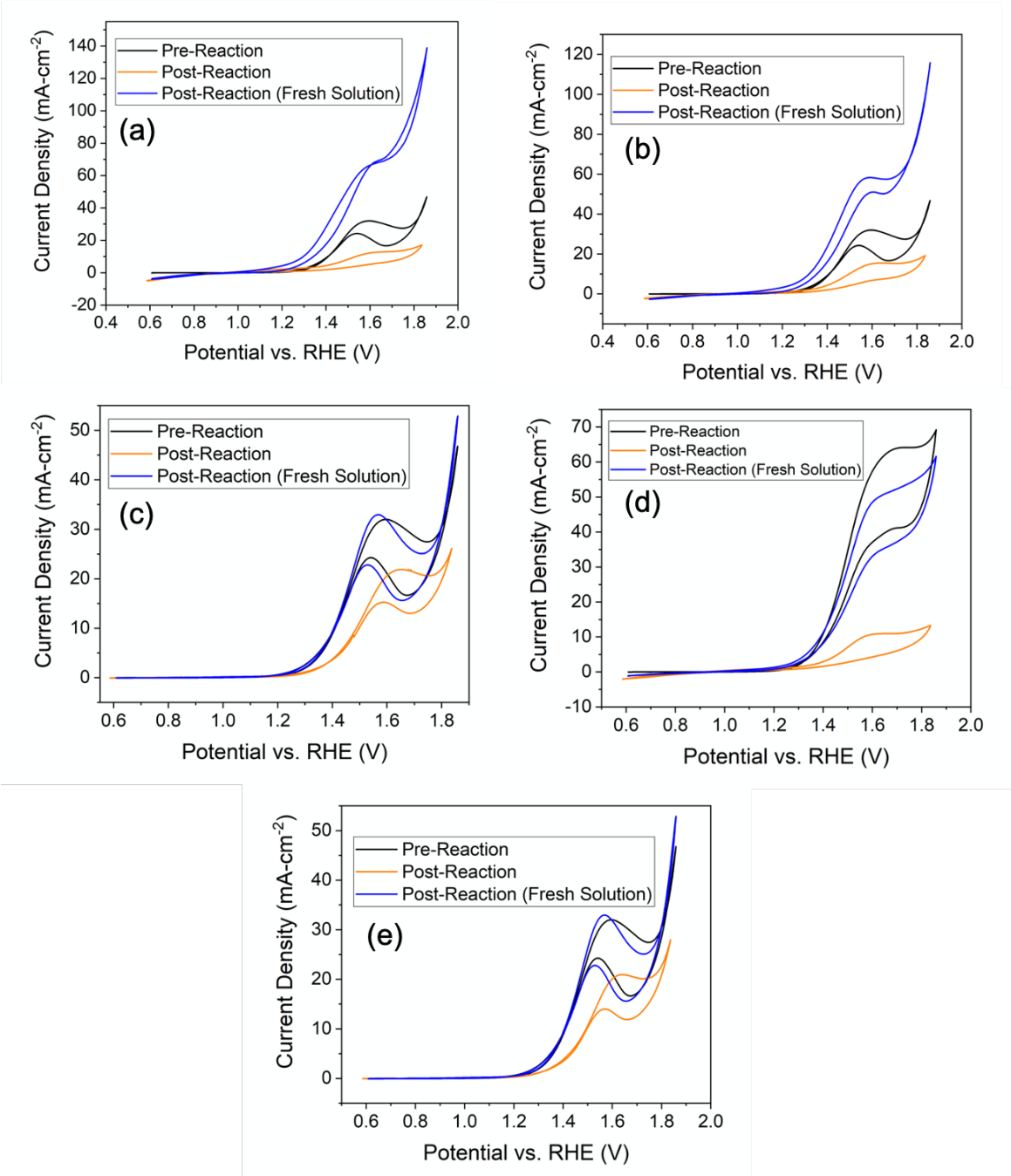

Fig. S10 Cyclic voltammetry performed at a scan rate of 50 mV-s^{-1} in 0.1 M glucose, 1.0 M NaOH (a-c,e) or 0.5 M NaOH (d) solutions. Starting glucose concentration was 0.1 M. Scans performed prior to the reaction (black), after a 30-hour chronoamperometry reaction in the same solution (orange), and in a new solution with the same electrode (blue) are all shown. Working electrode was Cu foil (2 cm^2) before (black) and after a 30-hour reaction (blue and orange) – reference and counter electrodes were Hg/HgO and platinum coil, respectively. All sets of data are taken from the 5th cycle of the scan. Reaction conditions forPanels a-e correspond to alphanumeric order from Table 1 in the main text.

The differences in Fig. S10 a-e require explanation. Triplicate analyses were performed for each of this conditions, i.e., the differences observed are not outliers. First, note the similarity between Panel c (Fig. 5 in the main text) and Panel e; further supporting the similarity between experiments when the Cu foil was pre-oxidized versus no pre-oxidation. For Panels a and b we noted enhanced cratering compared to Panel c after the experiments. Therefore, the increased current density in post-reaction cyclic voltammetry is explained by considering the increased surface area due to cratering.

Panel d, where the reaction was performed in 0.5 M NaOH, is the only experimental condition in which the peak current decreased for the post-reaction CV in a fresh solution. Relative to Panels a-c and e, the shape of the glucose oxidation peak in Panel d is different for pre and post-reaction scans. We suspect this behavior may be due to a dependence on the concentration of hydroxide in a E_rC_i' mechanism (a reversible electron transfer followed by an irreversible homogeneous chemical reaction), but lack of fundamental studies prevents further conclusions. We also note that, given the soluble copper species is suspected to be $Cu(OH)_4^{2-}$, a lower concentration of OH may lead to decreased solubility of copper and therefore less changes to copper surface morphology compared to the other conditions (equilibrium shifts left in $Cu + 4OH \leftrightarrow Cu(OH)_4^{2-}$). If $Cu(OH)_4^{2-}$ species play a role in the reaction, this equilibrium shift would decrease activity of the electrode towards glucose oxidation.

Recall from Fig. 4 that the reaction conditions for Panel c led to the highest yield for lactic acid. Panels a-d show that the pre-reaction current density is lower for Panel c; however, the post-reaction curve (orange) is higher for Panel c than any other condition. The stability of the electrode throughout the reaction could explain the high lactic acid yields.

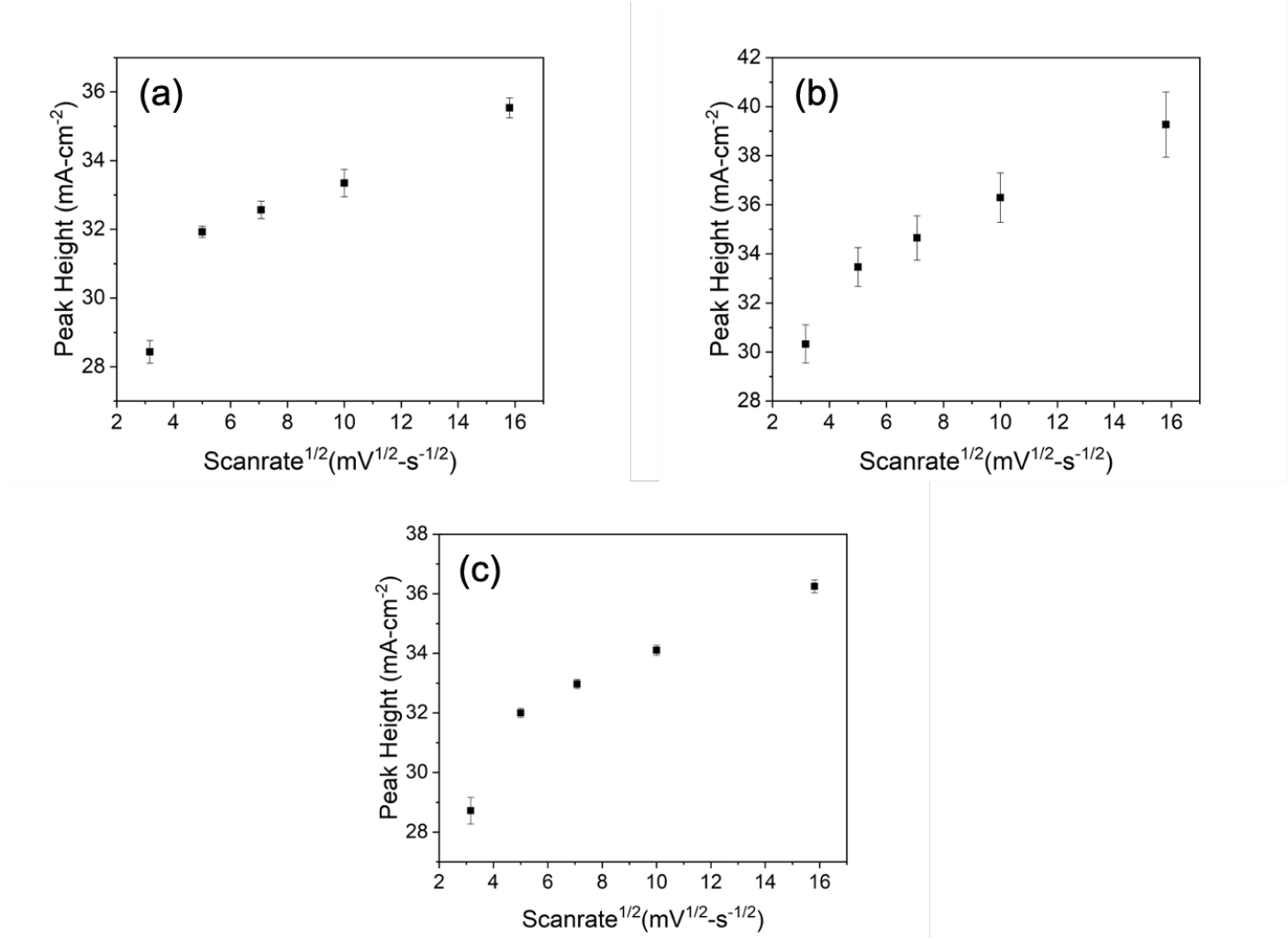

Fig. S11 Scan rate vs peak height experiments for 1.0 M NaOH (a), 0.5 M NaOH (b), and 1.0M KOH (c) solutions containing 0.1 M glucose. Working electrode was Cu foil (2 cm^2) after being oxidized for 1 hour; reference and counter electrodes were Hg/HgO and platinum coil, respectively.

In a traditional peak height vs scan rate set of experiments, a researcher would try and determine whether the system is kinetically or diffusion-limited by whether the system obeyed the Butler-Volmer equation (Equation 2) or the Randles-Sevcik equation (Equation 3), respectively.

$$i = FAk^0 C_i e^{(1-\alpha)f\left(E_{app}-E^0\right)} \quad (2)$$

Equation 2 - The Butler-Volmer equation where F is Faraday's constant, A is the area of the electrode, k^0 is the standard electron transfer rate constant, C_i is the concentration of the electroactive species i, α is the charge transfer coefficient, f is F/RT, R is the universal gas constant, T is the absolute temperature (K), E_{app} is the applied potential, and E^0 is the standard potential (thermodynamic theoretical required energy).

$$i_p = 0.4463\left(\frac{F^3}{RT}\right)^{0.5} n^{\frac{3}{2}} A D_0^{0.5} C_0^* v^{\frac{1}{2}} \quad (3)$$

Equation 3 – The Randles-Sevcik equation where F is Faraday's constant, R is the universal gas constant, T is the absolute temperature (K), n is the number of electrons per reaction, D_0 is the diffusion coefficient for the reacting species, C_O^* is the bulk concentration of reacting species, and υ is the scan rate.

By systematically varying the scan rate, the peak current should obey either Equation 2 or Equation 3. However, the equations only apply in systems with 1) reversible reactions and 2) simple mechanisms. While previous studies have tried to apply these equations to this system, neither of those assumptions apply and therefore conclusions as to kinetic or diffusion limitations are unwarranted from this type of study.

However, two linear regions appear in Fig. S11 and it is acceptable from these studies to conclude two different limiting mechanisms depending on the scan rate. Further insight as to the nature of these mechanisms is unwarranted from these experiments. In the cyclic voltammetry of prepared vs bare copper electrode section in the main text, we discussed two limiting mechanisms and these two regions could correspond to that idea, one region for each mechanism. However, this discussion from the main text as only data point (5 mV-s^{-1}) was recorded in the second region; therefore, conclusions about a second 'region' are unsupported by these data.

Turnover Frequency Calculations

Calculations were performed using the following formula:

$$\frac{molecules\ of\ glucose\ reacted}{active\ sites\ on\ copper\ surface * time}$$

Numerator was found from HPLC data, time was taken in seconds, and active sites of copper were found by considering the geometrical surface area and the crystal structure of a CuO [111] surface.

Comparison of Confidence Intervals

Conditions for potential-hold experiments were each performed three times. Confidence intervals between two means were found using the following formula:

$$z_x^* \sqrt{\frac{\sigma_1^2}{n_1} + \frac{\sigma_2^2}{n_2}}$$

where z_x^* is the coefficient for standard normal distribution for the desired confidence level (95% confidence interval - z_x^* = 1.96), σ_x is the standard deviation of sample set x, and $n_x$is the number of data points in sample set x (in our case, 3). If the difference between two values was greater than the confidence interval, the values were considered to have a statistically significant difference.

Stoichiometric Yield

Stoichiometric yields were calculated by considering the percentage of carbon atoms found in a specific analyte as compared to the total amount of carbons in the system from the starting concentration of glucose. In mathematical form:

$$\%Yield = \frac{n_i(\frac{C_i}{MW_i})}{6 * (\frac{C_{glucose,0}}{180.156\frac{g}{mol}})} x100\%$$

Where n_i is the number of carbon atoms found in i, C_i is the concentration of i (g-L^{-1}), MW_i is the molecular weight of i (g-mol^{-1}), and $C_{glucose,0}$ is the concentration of glucose just before the reaction began. The concentration of analytes in solution was calculated by a self-prepared calibration curve. All calibration curves had an $R^2 > 0.999$ for concentration ranges 0.7 to 17 mg-mL^{-1}.